Improved B_1-Mapping for Multi RF Transmit Systems

K. Nehrke[1], and P. Börnert[1]
[1]Philips Research Europe, Hamburg, Germany

Introduction

Accurate B_1-mapping is an essential prerequisite for multi-element transmit applications [1,2] like RF-shimming, supported by appropriate high-field MRI systems. However, MRI based B_1-mapping techniques potentially suffer from adverse error propagation in the range of small flip angles. For instance, multiple angle techniques [3] are compromised by the insufficient non-linearity between transmitted RF and received MR signal, making data fitting difficult. Moreover, steady-state techniques [4] are affected by the low steady-state characteristics at small flip angles. Also 180°-approaches [5] are difficult to realize in areas of low B_1. This potentially results in noisy or incomplete B_1-maps, and hence, in limited accuracy in regions with low B_1. Therefore, applications on multiple transmit systems like e.g. RF shimming may become difficult, because the RF field of each individual coil element typically penetrates only a limited spatial area. In the present study, this problem is addressed by employing suitable superpositions of coil elements to shift the B_1 field into a proper operational range of the mapping technique.

Methods

Experiments were performed on a 3T MRI system (Philips Medical Systems, Best, The Netherlands) equipped with eight transmit channels [6] and an 8-element TX/RX body coil [7]. The AFI (Actual Flip Angle Imaging) technique [4] was used for B_1-mapping (450 mm FOV, 128 scan matrix, alpha = 30°, TR_1 = 20 ms, TR_2 = 100 ms) in a cylindrical phantom (∅=400 mm). The modulus of the B_1-map was determined using the simple approximation given in [4]. The phase of the maps was directly taken from the AFI images. Assuming linear properties of the entire transmit system, the optimal RF waveforms can be determined by acquiring B_1-maps for N (= number of coil elements) linearly independent coil combinations, representing the basis functions of a fitting problem. In the present work, two different sets of basis functions were compared, in the following referred to as *single coil mode* and *inverted coil mode*, respectively. In the single coil mode, separate B_1-maps $m_i(x,y)$ were acquired for each coil element i, yielding directly the transmit sensitivities of the individual coil elements. In the inverted coil mode, complementary B_1-maps $\underline{m}_i(x,y)$ were acquired for eight different coil combinations, where all coils but one were enabled. The transmit sensitivities of the individual coil elements were calculated within a linear model (Eq. [1]) and compared with the B_1-maps acquired in the single coil mode.

$$m_i(x,y) = \frac{1}{N-1}\sum_{j=1}^{N} \underline{m}_j(x,y) - \underline{m}_i(x,y) \quad [1]$$

Results

Fig. 1 shows the B_1-maps for the individual coil elements. The maps clearly reflect the regular arrangement of the transmit coil array. The single coil mode results in B_1-maps suffering from strong noise in the regions of low B_1. In contrast, hardly any noise can be noticed in the maps derived from the inverted coil mode. In Fig. 2, selected profiles of the B_1-maps are shown as a graph for both modes. In the high B_1 regions, both curves are in good agreement, indicating a reasonable linearity of the transmit system. However, for flip angles smaller than 10°, the maps derived from the single coil mode are corrupted by noise. This is a result of the lower SNR of the source data and the adverse noise propagation of the AFI technique for small flip angles. In contrast, the maps based on the inverted coil mode are smooth for the entire B_1 range.

Discussion

As a result of the linearity of the transmit system, the coil basis functions used for multi-transmit applications (e.g. RF shimming) may be freely chosen. This may be utilized for adapting the RF field to a favourable operational range of the B_1-mapping technique. This potentially results in improved B_1-maps, as demonstrated in this work for the example of the AFI approach. In practice, basis functions with constructive superposition of the coil element sensitivities will be favourable. If reasonable estimates for the phases of the coil elements are not available, signal cancellation may occur and spoil the quality of the maps. In this case, the phases of the coil elements can still be estimated and proper B_1-maps can be acquired in a second iteration.

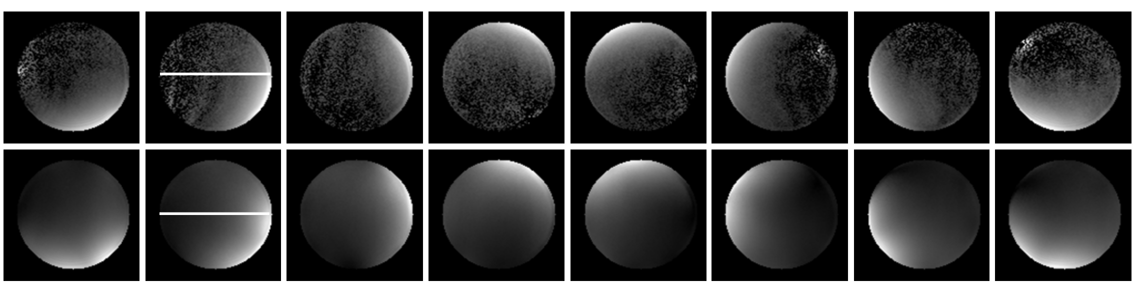

FIG. 1. B_1-maps are shown for the 8 individual transmit coil elements (from left to right). The maps were acquired in the single coil mode (top) and inverted coil mode (bottom), respectively. The latter results in strongly improved B_1-maps. The total measuring time was the same in both cases. The white straight lines indicate the profiles shown in Fig. 2.

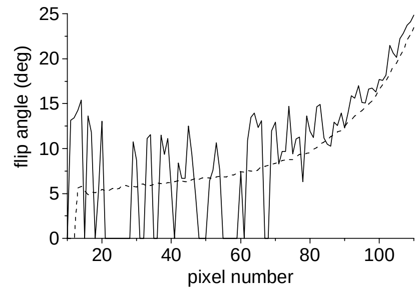

FIG. 2. B_1 profiles (cf. Fig.1) of coil element #2 acquired in different coil modes are shown (solid line: single coil mode, dashed line: inverted coil mode). Note the different noise characteristics.

References

1. Katscher U et al. Magn Reson Med. 2003;49(1):144-50.
2. Zhu Y. Magn Reson Med. 2004;51(4):775-84.
3. Cunningham CH et al. Magn Reson Med 2006;55:1326–1333
4. Yarnykh VL. Magn Reson Med. 2007;57(1):192-200.
5. Dowell NG, Tofts PS. Magn Reson Med. 2007;58(3):622-30.
6. Grässlin I et al., ISMRM 2006, p.129.
7. Vernickel P et al. Magn Reson Med. 2007;58:381-9.